Sun *et al.*
Chinese Journal of Mechanical Engineering (2024) 37:60
https://doi.org/10.1186/s10033-024-01016-6

Chinese Journal of Mechanical Engineering

ORIGINAL ARTICLE

Open Access

Multi-scale Modeling and Finite Element Analyses of Thermal Conductivity of 3D C/SiC Composites Fabricating by Flexible-Oriented Woven Process

Zheng Sun[1], Zhongde Shan[1*], Hao Huang[2], Dong Wang[2], Wang Wang[1], Jiale Liu[1], Chenchen Tan[1] and Chaozhong Chen[3]

Abstract

Thermal conductivity is one of the most significant criterion of three-dimensional carbon fiber-reinforced SiC matrix composites (3D C/SiC). Represent volume element (RVE) models of microscale, void/matrix and mesoscale proposed in this work are used to simulate the thermal conductivity behaviors of the 3D C/SiC composites. An entirely new process is introduced to weave the preform with three-dimensional orthogonal architecture. The 3D steady-state analysis step is created for assessing the thermal conductivity behaviors of the composites by applying periodic temperature boundary conditions. Three RVE models of cuboid, hexagonal and fiber random distribution are respectively developed to comparatively study the influence of fiber package pattern on the thermal conductivities at the microscale. Besides, the effect of void morphology on the thermal conductivity of the matrix is analyzed by the void/matrix models. The prediction results at the mesoscale correspond closely to the experimental values. The effect of the porosities and fiber volume fractions on the thermal conductivities is also taken into consideration. The multi-scale models mentioned in this paper can be used to predict the thermal conductivity behaviors of other composites with complex structures.

Keywords 3D C/SiC composites, Finite element analyses, Multi-scale modeling, Thermal conductivity

1 Introduction

Carbon fiber reinforced SiC matrix composites (C/SiC) have received increased attention across a number of disciplines in the fields of aerospace, high-speed vehicles, and thermo-structure construction due to their high thermal resistance, high specific stiffness and strength and lightweight [1]. The main challenge many researchers face is that 3D C/SiC composites could experience complicated mechanical and thermal conditions in huge temperature variation environments. Results from earlier studies demonstrate a strong and consistent association between the fatigue of the composites and the non-uniform thermal distributions [2–4]. To avoid potential failure and improve the utilization of the composites, it is essential to investigate the thermal conductivities of the 3D C/SiC composites.

Carbon fiber fabrics need to be prepared as reinforcement of 3D C/SiC composites at first. There are various manufacturing processes to produce three-dimensional fabric structures as preforms for textile composites. Traditionally, the textile preforms can be produced by

*Correspondence:
Zhongde Shan
shanzd@nuaa.edu.cn
[1] Nanjing University of Aeronautics and Astronautics, Nanjing 210016, China
[2] School of Mechanical Engineering, Beijing Institute of Technology, Beijing 100081, China
[3] CRRC Institute Corporation Limited, Beijing 100070, China

weaving, knitting, braiding, stitching and needle-punching. Weaving is the most widely used textile manufacturing technology and its process is suitable for making woven fabric textiles. Weaving offers a relatively low cost for mass production. Knitting is ideal for manufacturing components with complex shapes. A wide variety of complex net shape structures can be produced by the knitting process. Braiding is the most suited textile process for making highly complex, long and slender components that require high levels of conformability, torsional performance and structural integrity. Stitching is the simplest way of fabricating textile preform. However, it can cause significant in-plane fiber damage that may result in the degradation of in-plane mechanical properties of the composites. Needle-punching can inexpensively and produce complex net-shape preforms.

During the last decade, there has been a surge of interest in the investigation of the thermal conductivities of composites [5–7]. A considerable amount of literatures have been published on predicting the thermal conductivities of unidirectional (UD) composites by various theoretical models. Different formulas of Parallel and series [8], Charles [9], Bruggeman [10], Pilling [11], and Hatta and Taya [12] have been established to calculate the thermal conductivities of UD composites on the basis of many idealistic hypotheses. However, the main disadvantages of those formulas are that they are no longer suitable for other composites due to complex architectures and inhomogeneity of the composites.

Recently, a growing number of publications have focused on the finite element methods to obtain the thermal properties of various composites. Liu et al. [13] established a finite volume numerical model at three scale levels to predict the thermal conductivities of plain woven C/SiC composites based on 3D geometric reconstructions. The central cylinder and four 1/4 cylinders in the unit cell model of woven yarn, which is consisted of carbon fibers and SiC matrix, were built to obtain the thermal properties of the yarns. Dong et al. [14, 15] developed the multi-scale finite element analyses methods to investigate the thermal conductive behaviors of plain woven and 2.5D angle-interlock woven composites. At the microscale, they assumed that the fibers in the matrix impregnated fiber yarns were in hexagonal array distributions. Xu et al. [16] constructed fiber-scale and yarn-scale models to calculate the thermal conductivities of plain woven C/SiC composites. The effect of temperatures, thermal conductance and porosity were also studied. They selected the models with four semi-circles to calculate the properties of the yarns. Hassanzadeh-Aghdam et al. [17] delivered a new version of the semi-empirical Halpin-Tsai (H-T) model to investigate the influence of coating carbon nanotube on the effective thermal conductivities. The results showed that the coating significantly enhanced the nanocomposites' transverse thermal conductivities of CF-reinforced hybrid nanocomposites.

The voids are an important component in the composites, and have an essential influence on the thermal conductivities of various composites. More recently, studying voids has received continuing concern in modeling and analyzing. The methods can be classified into three categories, randomly selecting elements [18], building precise geometrical models [19], and constructing equivalent models [8]. Wei et al. [20] used a random function to select elements in the finite element models as void elements to study the effect of voids. They found that the random distribution of void defects had a little effect on the thermal conductivities, while void volume fraction significantly affected on thermal conductivities. Xu et al. [16] built a model with relatively precise locations, distributions and geometrical parameters to study the effect of porosity on thermal conductivity. Liu et al. [13] and Dong et al. [8] developed the void-matrix equivalent models to reflect the thermal properties of the matrix consisting of the voids. In addition, Wei et al. [21] and Zhou et al. [22] comparatively discussed the shapes, locations and arrangements of voids, and they found that the morphologies had almost no influence on thermal conductivity. In a whole, it can be found that multi-scale modeling methods are usually used to investigate the thermal properties of the composites at present. However, different composite forming processes lead to fiber package patterns, porosity and fiber volume fractions, few attentions have focused on the multi-scale finite element models that predict the thermal conductivities of 3D orthogonal C/SiC composites while simultaneously taking the fiber package patterns of microscale, porosity and fiber volume fractions into consideration. The effects of porosity, voids shapes, arrangements and sizes on thermal properties are unclear, limiting the 3D C/SiC composites application.

In the present work, the 3D orthogonal C/SiC composites are firstly woven by the flexible-oriented woven process and infiltrated via chemical vapor infiltration (CVI). Multi-scale modeling and finite element analyses are created to study the thermal conductivities of the composites. The local fiber volume fractions of yarns, the porosity and the geometrical parameters of each yarn, the thickness of interphase, and the sizes of mesoscale models are captured by X-ray computed tomography. In order to study the effect of fiber package pattern on the properties of yarns, the microscale models, including cuboid, hexagonal and fiber random distribution are developed. Besides, the effects of voids shapes, arrangements and sizes on thermal properties are comparatively analyzed by the void/matrix models. At the mesoscale,

the actual void morphology model, an equivalent model with void/matrix, and equivalent model with randomly selecting elements in the matrix are respectively built. The results from three mesoscale models are compared with the experiment values. Lastly, the effects of porosity and fiber volume fraction are also analyzed.

2 Flexible-Oriented Woven Process and Materials

Shan et al. [23, 24] innovatively proposed the flexible-oriented woven process (FOWP), based on the additive manufacturing principle. This process provides a completely new method to fabricate near-net-shape textile preforms with desired structural parts and required complex structure. The entire process is shown in Figure 1(a). In the present study, A PAN-based T300 3K carbon fiber (Nippon Toray, Japan) is used to fabricate the preform with a 3D orthogonal structure, shown in Figure 1(b). In addition, the guide sleeves are all replaced by fiber yarns. Subsequently, the preform is impregnated with a pyrolytic carbon (PyC) interphase and SiC matrix by means of a CVI process. The fiber volume fraction of the composites is approximately 46.9%.

The carbon fiber is considered as a transversely isotropic material [25], and the thermal conductivity is shown in Table 1. The property of the void is treated as the air [15]. Similarly, the interphase, voids, and SiC matrix are all viewed as isotropic materials. The thermal conductivities of SiC matrix are temperature dependent [2, 26], shown in Figure 1(c). Moreover, the thermal properties of carbon fiber, PyC interphase and voids are all independent of the temperature [16, 27], shown in Table 1.

3 Multi-scale Modeling

Multi-scale modeling and finite element analyses have been used to investigate the properties of composites [28–31]. Figure 2 illustrates the analytical procedures and some of the research results of the multi-scale modeling for predicting the thermal properties of the 3D C/SiC composites, and the downscale method is used to

Table 1 Thermal properties of constituent materials

		Carbon fiber	PyC interphase	Voids
Thermal conductivity (W/m/°C)	Longitudinal	7.81	25	0.023
	Transverse	1		

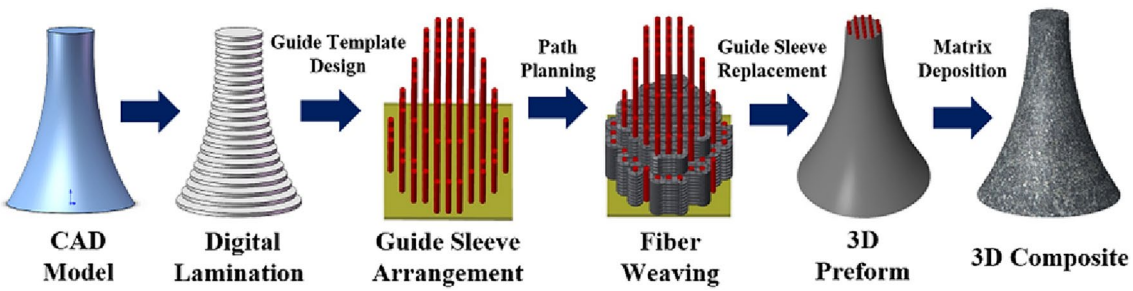

(a)

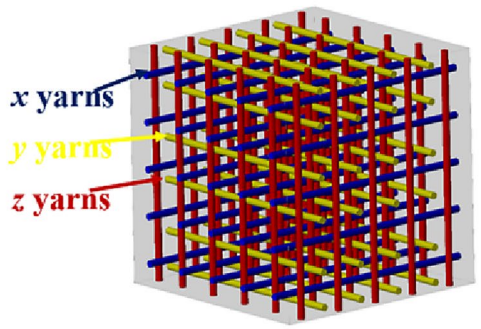

(b)

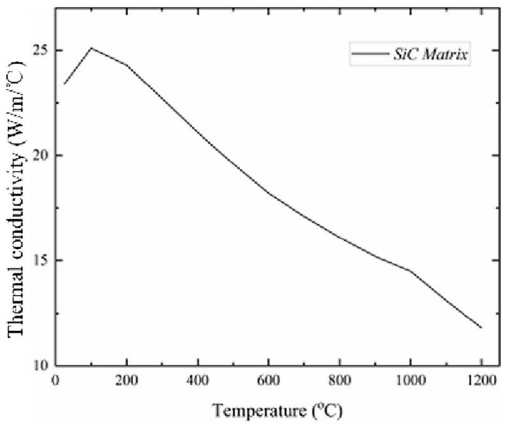

(c)

Figure 1 Scheme of flexible-oriented woven process and material parameters [2, 27]: **(a)** Flexible-oriented woven process, **(b)** Tomography of the preform, **(c)** Thermal conductivities of SiC matrix

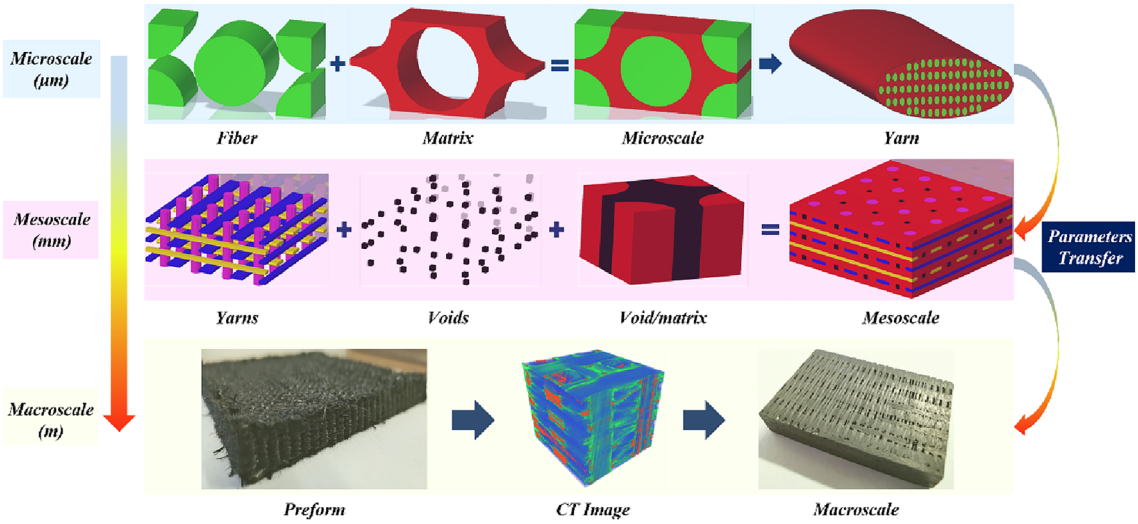

Figure 2 Multi-scale analyses framework of 3D C/SiC composites

calculate the equivalent thermal conductivity. In the framework of multi-scale analyses, the representative volume element (RVE) models are usually constructed owing to the spatial periodicity of the composites [32]. In this study, microscale, void/matrix and mesoscale RVE models are respectively developed. Microscale RVE models are structures containing a certain number of straight fibers within a given domain. The properties of the yarns are calculated by the microscale model. The voids exist inevitably during the matrix infiltration process and critically affect the properties of the composites [33]. Void/matrix equivalent models are built to obtain the properties of the SiC matrix with the voids. The mesoscale RVE model consists of fiber yarns and matrix, there are three kinds of RVEs in the 3D orthogonal structure: interior RVEs, surface RVEs and corner RVEs. Since the internal RVE plays a decisive role in the performance when the size is relatively large, only the internal RVE geometry is adopted to calculate equivalent performance. The material parameters of the mesoscale are obtained from the microscale and void/matrix models. The thermal properties of entire composites are reflected by the mesoscale RVE model.

3.1 Microscale Modeling

The fiber yarn materials parameters of the mesoscale model are from the microscale RVE models. The fiber package pattern and local fiber volume fractions of the yarns have great significant influence on the thermal properties of the fiber yarns. X-ray tomography technology (Sanying Precision Instruments Co., Ltd, Tianjin, China) is used to define the fiber volume fractions of the yarns by extracting the outline of the yarns. Three RVE models of cuboid, hexagonal and fiber random distribution are respectively developed. The Random Sequential Expansion method (RSE) algorithm [34] is applied to generate the fiber random distribution models. Figure 3 shows the finite element models of three RVE models.

Numerous X-ray images recording the yarns' geometrical parameters are processed to determine the local fiber volume fractions. The diameter of the carbon fiber is about 7 μm [15, 31]. The local fiber volume fractions are calculated by Eq. (1). Assumed that each yarn along different directions shares the same fiber volume fractions. The local fiber volume fractions of the yarn are 55%. Therefore, the geometrical parameters of the cuboid model are 8.4 × 8.4 × 8.4 μm, and the side lengths of the

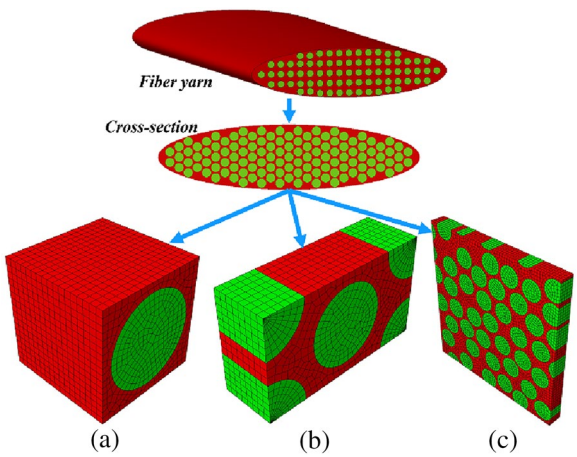

Figure 3 Finite element models of the microscale: (**a**) Cuboid RVE, (**b**) Hexagonal RVE, (**c**) Fiber random distribution RVE

hexagonal and fiber random distribution are respectively 15.6 × 9 × 5 μm, and 52 × 52 × 5 μm.

$$v_f = N \cdot \frac{\pi r_{fiber}^2}{A}, \tag{1}$$

where v_f is the local fiber volume fractions of the yarns, N stands for the numbers of the carbon fiber, which is defined by the materials manufacturers, r_{fiber} is the radius of the carbon fiber, and A represents the area of each yarn.

3.2 Void/Matrix Modeling

The porosity in composites is one of the critical manufacturing defects because it leads to variations in the thermal properties of the composites. The locations and distributions of the voids within the composites are irregular and random. Xu et al. [16] and our previous research [35] established a relatively accurate geometrical models of the voids. However, those precise models can't reflect the effect of the porosity on the thermal properties of the 3D C/SiC composites.

In order to perform research into the effect of porosity defects on thermal properties, it is necessary to determine the morphological characteristic of the voids. In this work, X-ray technology is used to obtain the geometrical parameters of the voids. The void/matrix RVE models are developed to obtain the thermal conductivities of the ceramic matrix including the voids. In order to systematically study the effect of void shapes, distributions, and locations on the thermal conductivity, six models are respectively built, shown in Figure 4. In addition, the void/matrix models with void volume fractions of 0, 5%, 10%, 15%, and 20% are respectively established to investigate the effect of porosity on the thermal conductivity of the composites. All the models share the same geometrical parameters. The sizes (length × width × height) are 3 × 3 × 3 mm.

3.3 Mesoscale Modeling

One of the strengths of the mesoscale RVE model in this study is that it represents a comprehensive consideration of the complex geometrical structures and the existence of the voids. The X-ray computed tomography reconstruction is applied to capture the geometrical parameters of the 3D C/SiC composites, the homogenization modeling approach is used in the mesoscale. The mesoscale RVE model consists of yarns and interphase along x, y and z direction, voids and SiC matrix. Supposing that the yarns and interphase are all straight in the model. Based on the periodicity of the composites and X-ray images, the sizes (length × width × height) of

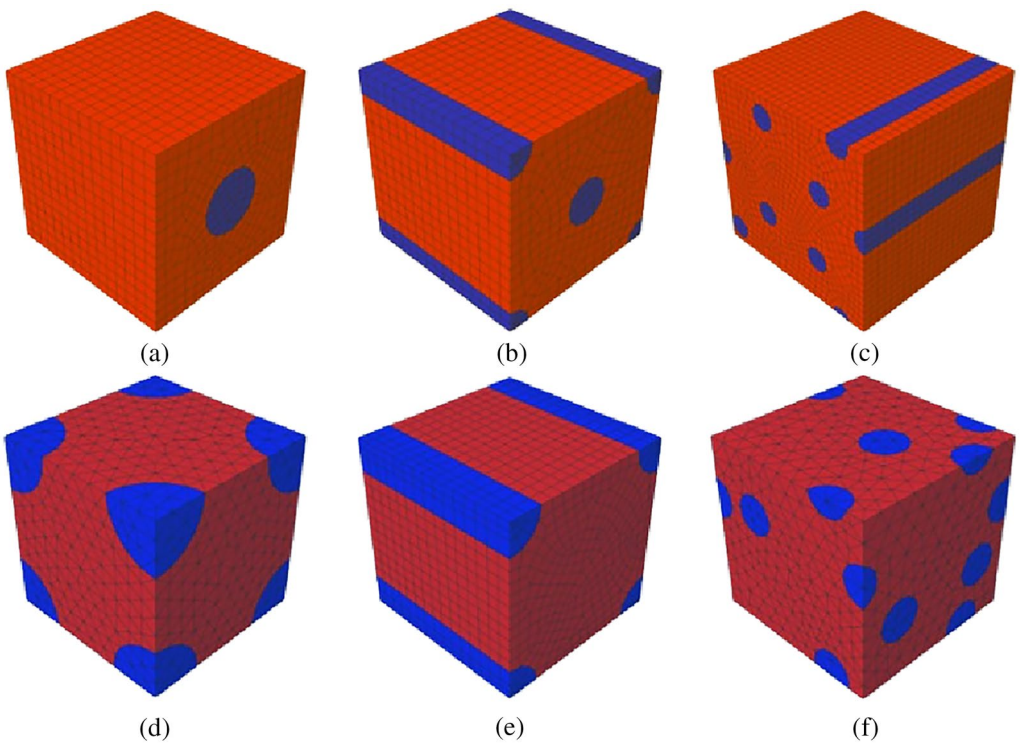

Figure 4 Finite element models of the microscale RVE: (**a**) Cylinder-center, (**b**) Cylinder-center-corner, (**c**) Cylinder random, (**d**) Sphere-corner, (**e**) Cylinder-corner, (**f**) Sphere-random

the mesoscale RVE model are 2.83 × 2.83 × 0.98 mm. The cross-section of three directions yarns is assumed as rectangular. The geometrical parameters are shown in Table 2. The fiber volume fraction is 47% under the geometrical parameter.

In order to investigate the effect of voids defects on the thermal conductivity of the 3D C/SiC composites, three RVE models are respectively built. The first model consists of yarns along three directions, interphase, SiC matrix and relatively precise shapes and locations of the voids, shown in Figure 5(a). The second model contains yarns along three directions, interphase and SiC matrix, shown in Figure 5(b). It is worth mentioning that the material parameters of the SiC matrix is dependent on the void/matrix models. The third model is composed of yarns along three directions, interphase and SiC matrix. Here a random function is employed to select elements from the matrix set as the void elements until the void volume fractions satisfy the threshold values. It must be noted that those elements which are identified as void defects are not moved away from the finite element model, but those material parameters of those elements are considered as air. The void defects in the matrix set are highlighted as "black", as shown in Figure 5(c).

Table 2 Geometrical parameters of the mesoscale RVE model

	Sizes of *x* yarn (mm)	Sizes of *y* yarn (mm)	Sizes of *z* yarn (mm)	Thickness of interphase (mm)	Porosity (%)
Values	1.32 × 0.33	1.32 × 0.33	1.17 × 1.07	0.03	24

The computer-aided-engineering (CAE) software SOLIDWORKS (ver. 2015) is used to build the mesoscale RVE model. Then, the model is translated to another powerful pre-processing for finite element meshing software Hypermesh (ver. 2013) to obtain a good quality mesh. Due to the periodic temperature boundary conditions mentioned in the next section requiring the corresponding nodes to be paired, the grids should be periodic spatially. Duplicating 2D grids along the opposite surfaces is carried out. The 3D grids are meshed on

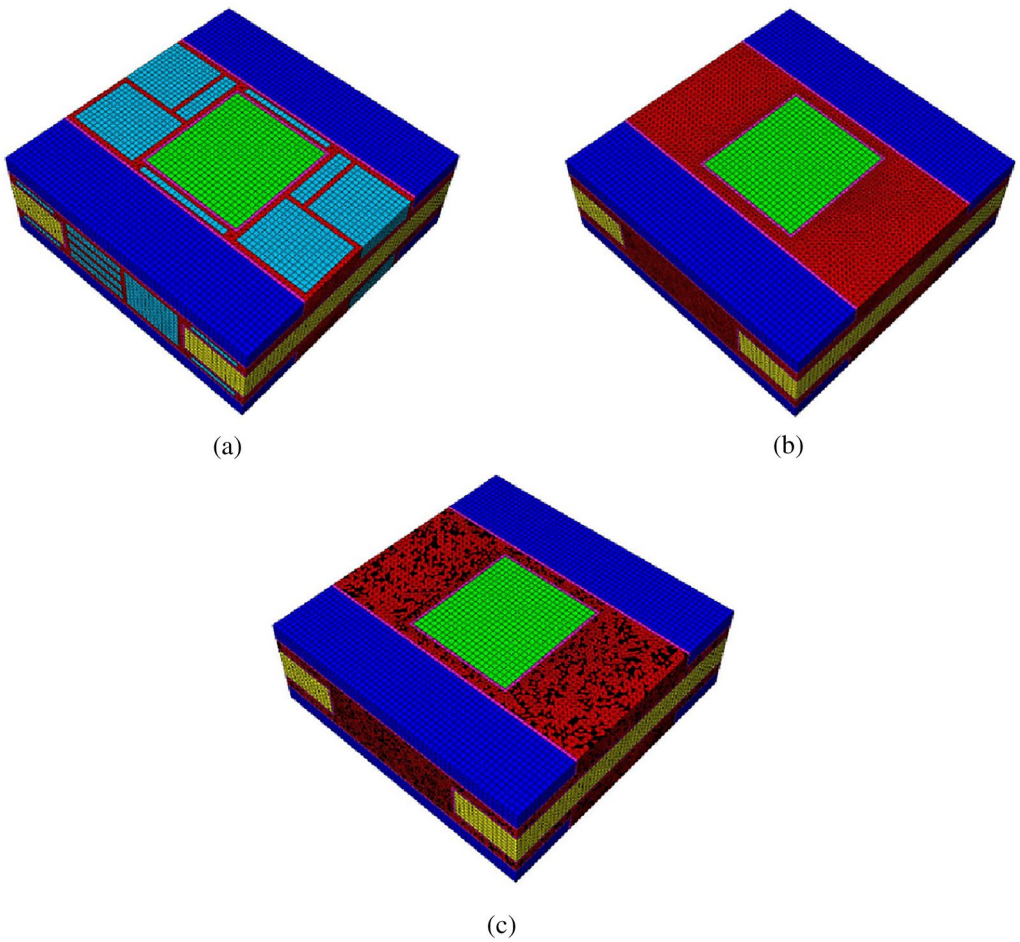

Figure 5 Finite element model of mesoscale RVE model: (**a**) Mesoscale model with actual voids distribution (blue), (**b**) Mesoscale model with void/matrix equivalent model (red), (**c**) Mesoscale model with random void distribution elements (black)

the basis of 2D grids. Therefore, the yarns, voids and matrix respectively are discretized by DC3D4, DC3D8 and DC3D8 of ABAQUS thermal solid elements. In addition, the yarns are viewed as transversely isotropic entities and the material orientations are assigned by three local coordinates. After checking the mergence, the present mesh size of the mesoscale model was set as approximately 0.05. The whole model displayed contains 136035 elements and 73999 nodes.

4 Finite Element Analyses

4.1 Periodic Temperature Boundary Conditions

In order to obtain continuous temperature and uniform heat flux distribution, the periodic temperature boundary conditions (PTBC) are commonly used to calculate the thermal properties of the RVE models [36]. Figure 6 shows the illustration of the node locations and node numbers of the PTBC in a cuboid cell. As is shown in Figure 6, P_{x+}, P_{x-}, P_{y+}, P_{y-}, P_{z+}, and P_{z-} are pairs of periodic nodes on the opposite parallel surfaces and these linked lines are parallel to three coordinate axes, respectively. According to the PTBC, the constraint equations can be applied on the nodes of the faces, edges and vertexes [37]. In the present study, the constraint equations of edges are taken as an example here. The cases of faces and vertexes can be concluded by reference to the edge equations.

For the edges excluding vertexes, twelve edges can be classified into three groups, Edges *IX*, *X*, *XI* and *XII* (dark red) are parallel to *x* axis. Edges *V*, *VI*, *VII* and *VIII* (dark blue) parallel the *y* axis. Edges *I*, *II*, *III* and *IV* (green) are parallel to *z* axis. The constraint equations are summarized as:

$$\begin{aligned} &T_{II} - T_I - T_2 = 0, \quad T_{III} - T_{IV} - T_2 = 0, \quad T_{IV} - T_I - T_4 = 0, \\ &T_{VI} - T_V - T_2 = 0, \quad T_{VII} - T_{VIII} - T_2 = 0, \quad T_{VIII} - T_V - T_5 = 0, \\ &T_X - T_{IX} - T_4 = 0, \quad T_{XI} - T_{XII} - T_4 = 0, \quad T_{XII} - T_{IX} - T_4 = 0, \end{aligned} \tag{2}$$

where T is the temperature, 1, etc. are the vertexes which corresponds to the point A, etc. in Figure 6, and *I*, etc. are the edges. Eq. (2) can be applied by defining the linear multi-point constraint equations in ABAQUS.

4.2 Governing Equations

The 3D steady-state finite element analyses are conducted on the RVE models to obtain the temperature and heat flux. The governing equations are described as:

$$\begin{aligned} k_{xx}\frac{\partial^2 T}{\partial x^2} + k_{yy}\frac{\partial^2 T}{\partial y^2} + k_{zz}\frac{\partial^2 T}{\partial z^2} + \left(k_{xy} + k_{yx}\right)\frac{\partial^2 T}{\partial x \partial y} \\ + \left(k_{yz} + k_{zy}\right)\frac{\partial^2 T}{\partial y \partial z} + \left(k_{xz} + k_{zx}\right)\frac{\partial^2 T}{\partial x \partial z} = 0. \end{aligned} \tag{3}$$

Where T is the temperature, x, y and z stand for the different directions, k_{xx}, k_{yy}, k_{zz}, k_{xy}, k_{yx}, k_{yz}, k_{zy}, k_{xz}, and k_{zx} are the thermal conductivity along various directions, which can be considered as being transversely isotropic for the carbon fiber and isotropic for the matrix. Next, the thermal conductivity can be calculated by Fourier's Law [13]:

$$q_{ii} = k_{ii}\nabla T_{ii}. \tag{4}$$

Where q_{ii}, k_{ii} and T_{ii} are heat flux density, the thermal conductivity and temperature gradient in *ii* direction (*ii*=*xx*, *yy* and *zz*), respectively.

In conclusion, the procedures of calculating thermal conductivity of the 3D C/SiC composites are summarized as follows:

I. The PTBC is applied to the RVE models through the finite element software ABAQUS.
II. 3D steady-state finite element steps are carried out to obtain the heat flux density and temperature contour.
III. The effective thermal conductivity of the RVE models is calculated by Eq. (4).

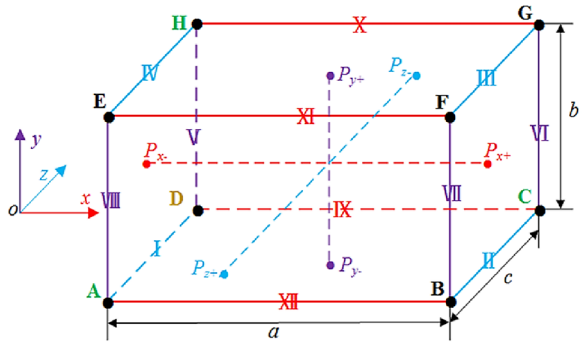

Figure 6 Illustration of periodic temperature boundary conditions for the cubic unit cell

4.3 Finite Element Method

Admittedly, there are two categories of thermal analyses: steady state and transient state. In the steady state analyses, the heat flux is measured to obtain the thermal conductivities. For the transient state steps, the thermal diffusivity is first achieved and then the thermal conductivities are calculated. In this work, the steady state

analyses are applied to acquire the thermal conductivities of each RVE model. Although the steady state steps do not directly simulate the experimental processes, it does provide a valid benchmark for the thermal diffusivity calculations in parallel with a transient solution. In addition, the steady state analysis confirms the integrity of the model's volumetric continuum generated from the morphological data.

It is well known that the contact property existed at the interfaces between two different materials has a significant influence on the final thermal conductive values [8, 14]. This paper doesn't focus its attention on the interface thermal contact behaviors. In addition, the effect of the convection and radiation are ignored. Therefore, the 'surface-to-surface' contact is defined between two different materials. The thermal contact resistance with no pressure is defined among the yarns, interphase and matrix. The values of contact thermal conductivity are assumed to be about 2.4×10^7 W/m/ºC [26, 38], and wouldn't change as temperature increases.

5 Results and Discussion

5.1 Microscale RVE Model

Here the effect of fiber package pattern on the thermal conductivities of the microscale is firstly discussed. The thermal conductivities of cuboid, hexagonal and fiber random distribution RVE models with 55% fiber volume fraction at different temperature points are shown in Figure 7(a). It can be inferred that there is a transition point at temperature of 100 °C. The values will increase slightly from room temperature to 100 °C. When the temperature is above 100 °C, the thermal conductivities will decrease with increasing temperature. Since the thermal conductivity of the resin matrix is always greater than fibers under the imposed boundary conditions, the SiC matrix plays a leading role in the heat transfer process. The thermal conductivities of the matrix reached the maximum at the temperature of 100 °C, which induces the thermal conductivities of the C/SiC composites appear a maximum value at the temperature of 100 °C, as shown in Figure 7(a). In addition, since the thermal conductivity of the SiC matrix is higher than the thermal conductivity of the fiber, the heat is mainly transferred through the matrix, which is continuously distributed in the longitudinal direction of each model, and the overall distribution is more uniform. Therefore, the equivalent thermal conductivity is independent of the fiber distribution, and the longitudinal thermal conductivities of three models are almost same. However, the transverse thermal conductivities of hexagonal RVE are slightly larger than the cuboid and fiber random distribution RVE. Therefore, it can be concluded that the fiber package pattern has little effect on the thermal conductivities of the microscale models.

In order to reduce computation time and lower model difficulty, the cuboid RVE model is used to study the effect of fiber volume fractions on the thermal conductivities. To determine the influence of fiber volume fractions of the microscale on the thermal conductivities, the cuboid RVE models with fiber volume fractions of 45%, 50%, 55%, 60%, 65%, 70% and 75% are built, respectively. The results related to different fiber volume fractions are shown in Figure 7(b). It can be concluded that both longitudinal and transverse thermal conductivities decrease as fiber volume fractions increase. Notably, the longitudinal thermal conductivities decrease by 28.03% when the fiber volume fractions increase from 45% to 75% at room temperature. Similarly, the transverse thermal conductivities

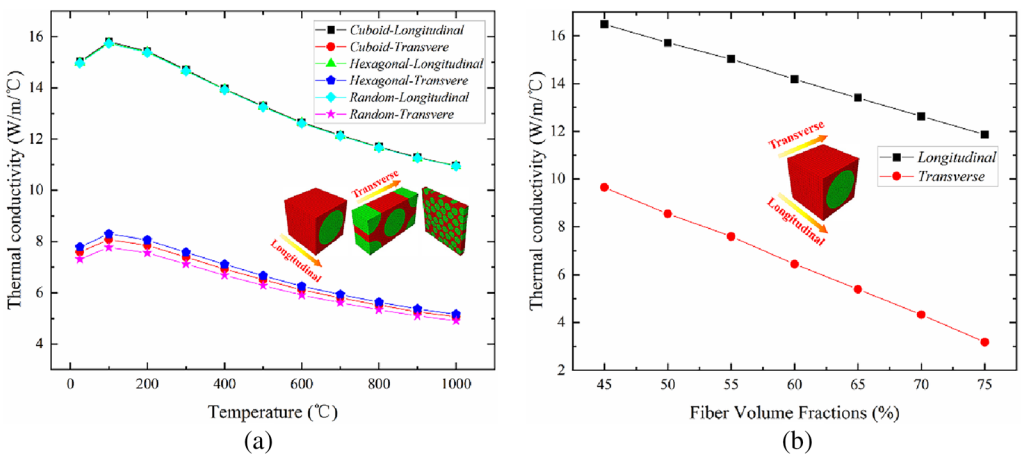

Figure 7 Thermal conductivities of microscale models: (**a**) Thermal conductivities of cuboid, hexagonal and random RVE models, (**b**) Thermal conductivities of cuboid RVE with different fiber volume fractions

decrease by 67.04%. The fiber volume fractions of the microscale RVE models have great effect on the transverse thermal conductivities than the longitudinal ones.

5.2 Void/Matrix RVE Model

From the information of X-ray images, the distribution and shape of the voids are irregular. In order to investigate the effects of void sizes, locations and shapes on the thermal conductivities of the void/matrix RVE models, six models containing of different void morphological characteristics are respectively developed in 3.2, including cubic models of cylinder-center, cylinder-center-corner, cylinder random, sphere-corner, cylinder-corner, and sphere-random. It must be emphasized that each model shares the same void volume fraction. Figure 8(a) shows the variations of the thermal conductivities with different voids characteristics. It can be found that the results of thermal conductivities agree well with each other, which demonstrates that the morphological characteristics of voids have little influence on the thermal conductivities. Hence, the cylinder-center cubic model is used to calculate the thermal conductivities with different void volume fractions.

To determine the effect of porosity on the thermal conductivities, void/matrix RVE models with porosities of 10%, 20%, 24%, 30%, 40% and 50% are established, respectively. The thermal conductivities associated with different porosities and temperatures are shown in Figure 8(b). It can be obviously seen that there is a transition point at temperature of 100 °C. From room temperature to 100 °C, the thermal conductivities of void/matrix models slightly increase. The values begin to decrease when the temperature is above 100 °C. As for the longitudinal heat transfer process, the heat is mainly transferred through the SiC matrix. And since the nonlinearity of the thermal conductivity of the SiC matrix with temperature, there is also a transition point at temperature of 100℃ in Figure 8(b). More importantly, the thermal conductivities of void/matrix RVE models decreases with increasing porosity. The voids are effective in lowering the thermal conductivities of the model. In particular, the thermal conductivities of the void/matrix RVE model decrease by 38.68% when the porosity increases from 10% to 50% at the temperature of 100 °C.

5.3 Mesoscale RVE Model

Accordingly, the thermal properties of matrix and fiber yarns in the mesoscale RVE model are from the void/matrix and microscale models, respectively. A Hot Disk TPS 2500S Thermal Constants Analyzer (Göteborg, Sweden) based on the transient plane source method is used to measure the thermal conductivity of the composites. The sample size is 20 mm × 16 mm × 5 mm, which is machined through the in-plane and out-of-plane directions. The temperature and response time of the tensor are recorded to calculate the thermal conductivities of the samples. The numerical results, in which the properties of the matrix are obtained from the void/matrix RVE model, and experimentally determined values are shown in Table 3. The data reveal a close coincidence between the two sets of the values, which validates the accuracy of the mesoscale RVE models. Furthermore, the numerical and experimental results indicate that the in-plane and out-of-plane thermal conductivities increase moderately from room temperature up to 100 °C. When the temperature is above 100 °C, there is an opposite trend between the in-plane and out-of-plane thermal conductivities.

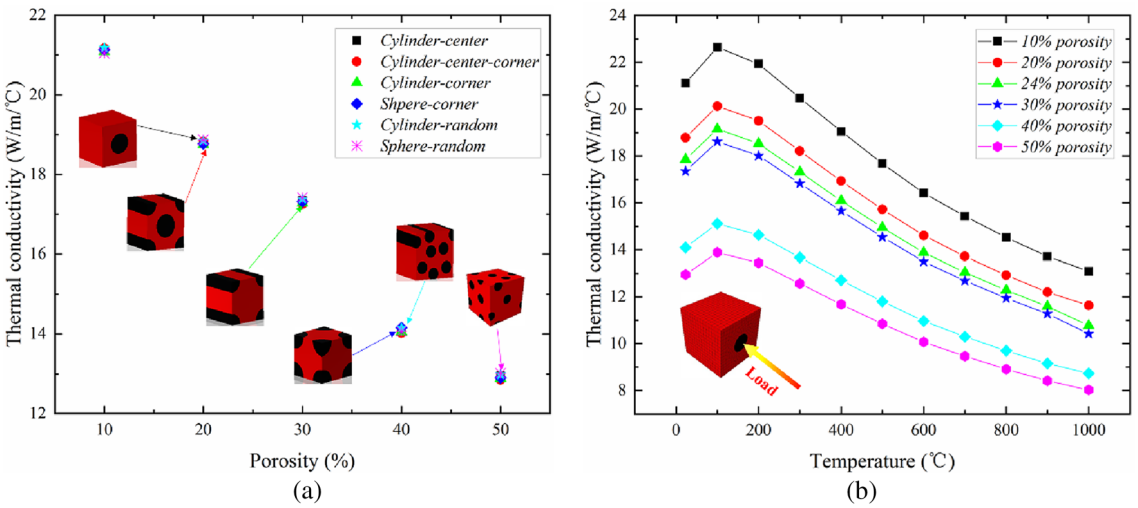

Figure 8 Thermal conductivities of void/matrix: (**a**) Thermal conductivities of the model with different morphological characteristics of voids, (**b**) Thermal conductivities at different temperatures and various porosities

Table 3 Experimentally determined and predicted thermal conductivities of 3D C/SiC composites

Temperature (°C)	In-plane (W/m/°C)		Error (%)	Out-of-plane (W/m/°C)		Error (%)
	Experiment	Prediction		Experiment	Prediction	
23	12.32	14.35	16.48	12.70	13.39	5.43
100	13.49	15.16	12.31	13.79	14.18	2.83
200	13.87	14.77	6.49	13.16	13.81	4.94
300	12.16	14.00	15.13	12.64	13.06	3.32
400	11.69	13.22	13.09	12.01	12.30	2.41
500	11.25	12.51	11.20	11.45	11.61	1.40
600	10.63	11.83	11.29	10.39	10.95	5.39
700	10.17	11.30	11.11	10.02	10.43	4.09
800	9.45	10.81	14.39	9.84	9.95	1.12
900	9.13	10.38	13.69	9.08	9.52	4.85
1000	8.42	9.92	17.81	8.67	9.10	4.96

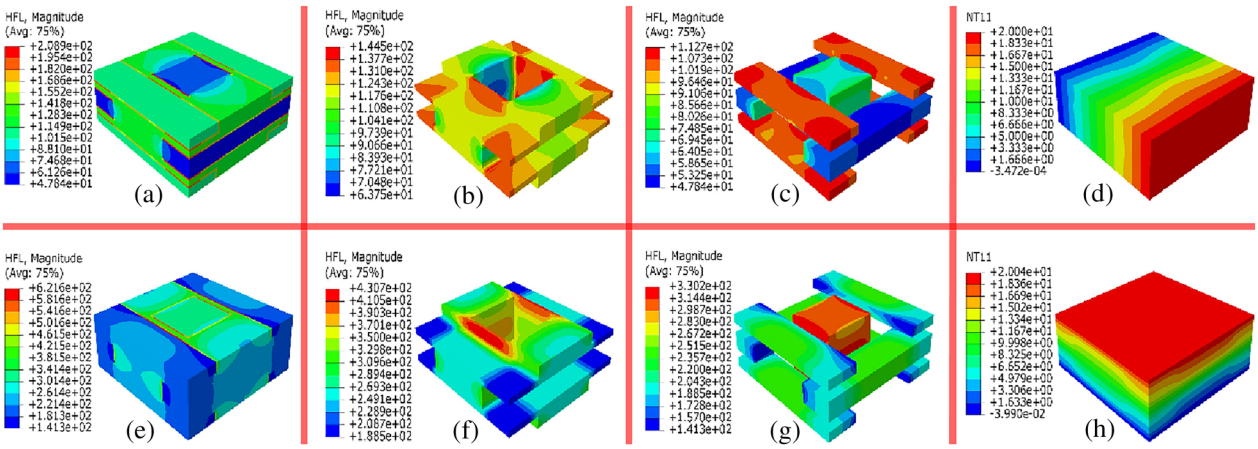

Figure 9 Heat flux distribution and temperature fields of mesoscale RVE model: (**a**–**d**) In-plane direction, (**e**–**h**) Out-of-plane direction

In addition, the heat flux distribution and heat fields in the in-plane and out-of-plane directions of the mesoscale RVE model at room temperature are shown in Figure 9, respectively. It can be easily seen that the yarns in parallel with the load transfer the heat while the other yarns hinder the heat flow. In addition, in the in-plane and out-of-plane direction, the heat flux in the interphase is always higher than other parts in the mesoscale RVE model. This is simply because the interphase volume ratio is the lowest and the thermal conductivities of the interphase are more prominent than that of yarns and matrix. Besides this, from the Figure 9(d) and (h), it can be concluded that the in-plane and out-of-plane temperature fields are uneven.

In order to comparatively study the effect of mesoscale model with void/matrix, equivalent model and random void distribution elements on the thermal conductivities, the predicted thermal conductivities are shown in Figure 10. The thermal conductivity of the resin matrix

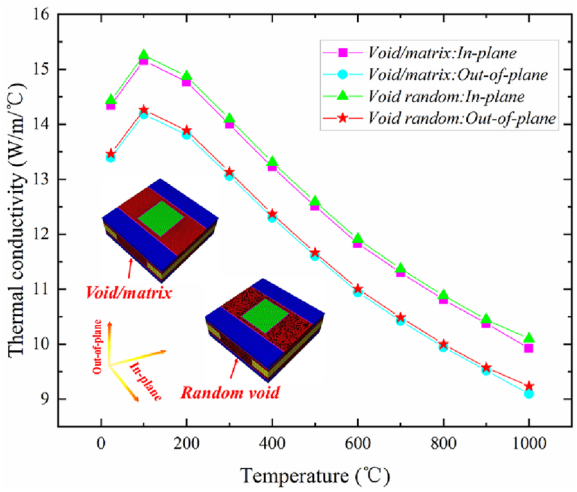

Figure 10 Comparison of thermal conductivities of mesoscale RVE with void/matrix model and random void distribution model

is always greater than fibers under the imposed boundary conditions, while the thermal conductivity of the PyC interface, although higher than that of the matrix, will only result in a greater heat flow density at the interface due to the lower volume fraction, as shown in Figure 9. Considering the magnitude of the thermal conductivity values and the volume fraction of each component of the model material, matrix plays a leading role in the heat transfer process. So the same principle leads to the nonlinearity of the thermal conductivity of the mesoscale model with temperature. A comparison of the two results reveals that there are not many differences between the two models. This finding broadly supports that both mesoscale RVE models proposed in this paper can be used to calculate the thermal conductivities of the 3D C/SiC composites. Consequently, the mesoscale RVE model with void/matrix equivalent model is adopted to investigate the effect of porosity on the thermal conductivities of the 3D C/SiC composites in next section.

5.4 Effect of Porosity on Thermal Conductivity

Previous researches [16, 22, 35] have reported that the porosity has a significant influence on the thermal conductivity behaviors of the composites. In this section, five mesoscale models with cylinder-center cubic are built to investigate the thermal conductivities with 10%, 20%, 30%, 40%, and 50% porosities at room temperature. Figure 11 shows the variations of the in-plane and out-of-plane thermal conductivities with a change in the porosity from 10% to 50%. It is evident that both sets of thermal conductivities decrease with increasing porosity. When the porosity increases from 10% to 50%, the in-plane and out-of-plane thermal conductivities drop by 20.19% and 17.20%, respectively. This phenomenon indicates that the porosity has a great effect on the in-plane and out-of-plane thermal conductivities.

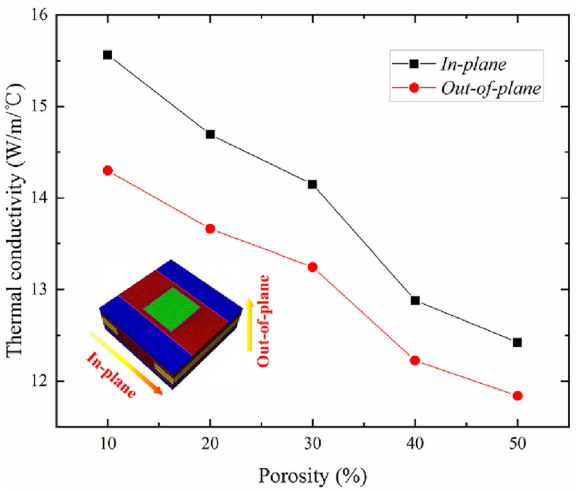

Figure 11 Schematic of thermal conductivities with various porosities

The heat flux and temperature along in-plane and out-of-plane directions are extracted to describe the variation of the thermal conductivity behaviors inside the 3D C/SiC composites under different porosities. As is shown in Figure 12, the *Line-1* and *Line-2* including 11 equal interval points are extracted from the edges of the mesoscale RVE models along in-plane and out-of-plane directions, respectively. In order to obtain the heat flux distribution and temperature fields, a 20 °C temperature gradient (20 °C in high temperature surface and 0 °C in low temperature surface) is imposed on the mesoscale RVE models. Heat flux distribution and temperature fields are shown in Figure 12. It can be seen that both in-plane and out-of-plane heat flux present a normal distribution from Figure 12(a) and (b). The heat flux values within the SiC matrix are always larger than that in the yarns. More importantly, there is a substantially increase at the intersection of yarns and matrix. The heat flux will reach the maximum in the middle of the RVE model. Additionally, the values of heat flux along in-plane and out-of-plane directions decrease with the increment of the porosities ranging from 10% to 50%. As is shown in Figure 12(c) and (d), it can be inferred that the temperature fields are almost unchanged as porosities increase both in in-plane and out-of-plane directions. Consequently, the porosities have a significant effect on the heat flux distribution and have very little impact on the temperature fields.

5.5 Effect of Fiber Volume Fraction on Thermal Conductivities

As mentioned in Section 2, the various fiber yarns can be used to replace the guide sleeves during the FOWP, i.e., 1K, 3K, or 6K fiber yarns. The fiber volume fractions along the out-of-plane direction could be decided and designed. Therefore, a study considering the dependence of the thermal conductivities on the fiber volume fractions along the out-of-plane direction is necessary. Four additional mesoscale models with 5%, 8%, 10% and 12% fiber volume fractions are built by changing the geometrical parameters of the cross-sections of out-of-plane yarns. In addition, the fiber volume fractions along the out-of-plane direction of the origin mesoscale model are 15.6%. The predicted thermal conductivities of the 3D C/SiC composites with various fiber volume fractions are presented in Figure 13 at room temperature. It is obviously concluded that the in-plane thermal conductivities are always more significant than the out-of-plane thermal

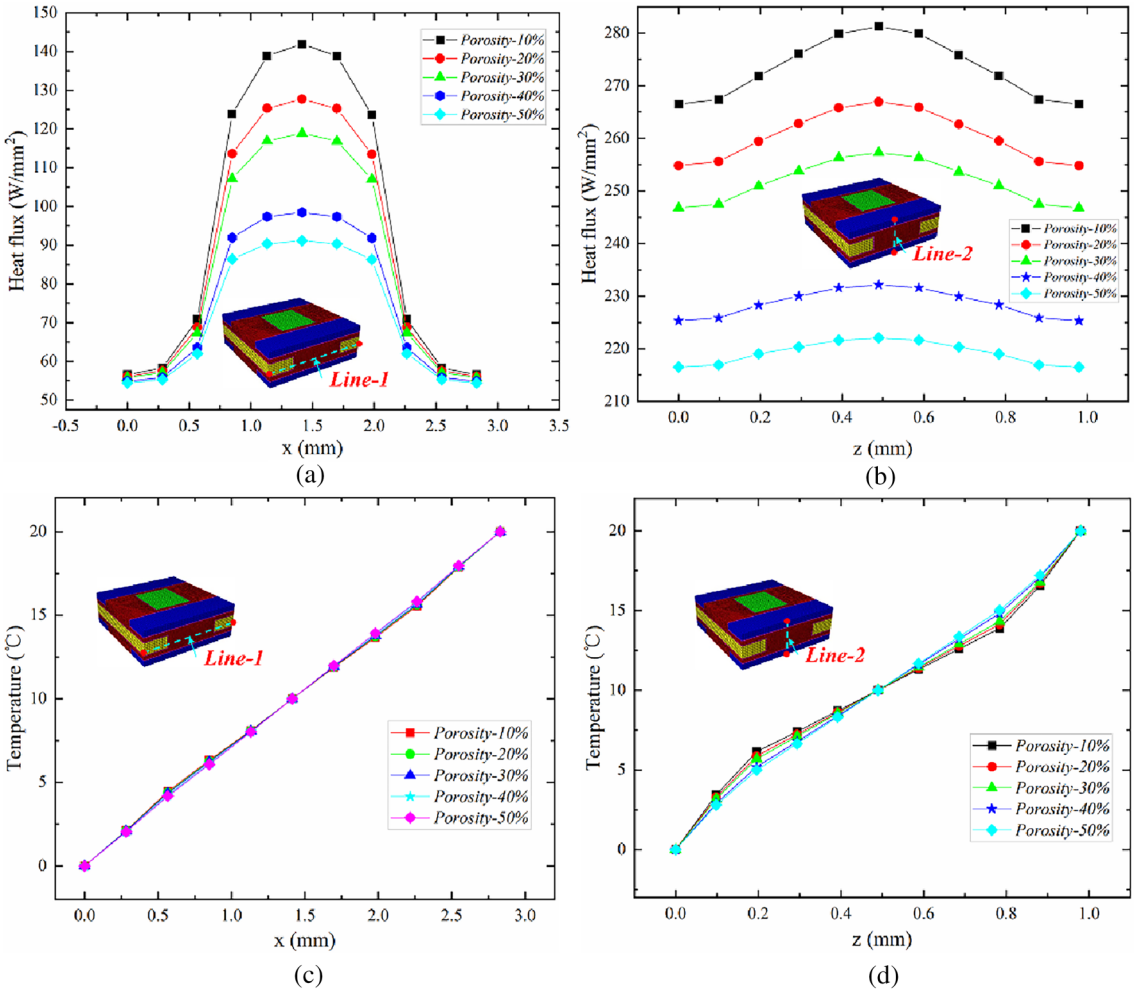

Figure 12 Schematic of heat flux and temperature distribution with various porosities: (**a**) Heat flux along in-plane direction, (**b**) heat flux along out-of-plane direction, (**c**) Temperature distribution along in-plane direction, (**d**) Temperature distribution along out-of-plane direction

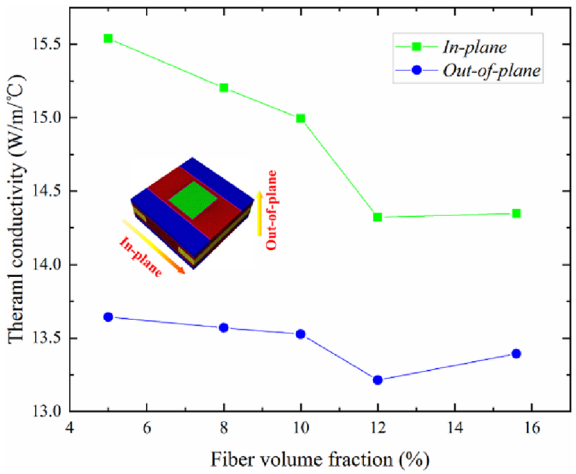

Figure 13 Schematic diagram of thermal conductivities of 3D C/SiC composites with different fiber volume fractions

conductivities with the increment of the porosities ranging from 5% to 15.6%.

Furthermore, the results show that the in-plane and out-of-plane thermal conductivities of the 3D C/SiC composites decrease with fiber volume fractions increase when the fiber volume fractions are under 12%. The in-plane thermal conductivities decrease by 7.85% when the fiber volume fractions increase from 5% to 12%. Similarly, the out-of-plane thermal conductivities descend by just 3.14%. In contrast, there is a moderate upward trend of the thermal conductivities along in-plane and out-of-plane directions, where the fiber volume fractions are more than 12%. Particularly, this phenomenon suggests that the designative thermal conductivities could be achieved by selecting appropriate fiber volume fractions for the different directions.

6 Conclusions

A multi-scale modeling and finite element analysis of thermal conductivities of 3D C/SiC composites have been carried out at temperatures ranging from room temperature to 1000 °C in this study. The results of the RVE models correspond closely to the experiment. In addition, the porosity and fiber volume fraction is also taken into consideration. The present study establishes a relatively complete framework for predicting the thermal conductivity behaviors of 3D C/SiC composites. The following conclusions are summarized:

(1) The fiber package pattern has little effect on the thermal conductivities of the microscale models. The simplest microscale RVE model, cylinder-center, can be used to achieve the thermal properties of each yarn.
(2) The morphological characteristics of voids have little influence on the thermal conductivities. The thermal conductivities of the matrix including voids can be calculated by the void/matrix RVE model with cylinder-center cubic.
(3) The experimental thermal conductivity test results are in good agreement with the corresponding mesoscale RVE simulation results. The porosity has a great effect on the in-plane and out-of-plane thermal conductivities. Furthermore, the designative thermal conductivities could be achieved by selecting appropriate fiber volume fraction for the different directions.

The model established in this study is based on an idealized geometric structure, particularly at the mesoscale level, disregarding the influence of real yarn conditions and defects. This omission can introduce certain inaccuracies in the prediction of thermal conductivity. Therefore, more influence factors on thermal conductivity will be considered in our future work, which includes actual geometrical structure, processing parameters and interface. Moreover, multi-scale modeling and finite element analyses of 3D C/SiC composites can be applied in 3D composites damage analysis.

Acknowledgements
Not applicable.

Authors' Contributions
ZS wrote the manuscript and was in charge of the whole trial; ZDS supervised the whole work of this paper; HH and DW assisted geometric modeling and numerical simulation; WW, JLL, CCT and CZC assisted review and editing. All authors read and approved the final manuscript.

Funding
Supported by Science Center for Gas Turbine Project of China (Grant No. P2022-B-IV-014-001), Frontier Leading Technology Basic Research Special Project of Jiangsu Province of China (Grant No. BK20212007), and the BIT Research and Innovation Promoting Project of China (Grant No. 2022YCXZ019).

Data Availability
Data will be made available on request.

Declarations

Competing Interests
The authors declare that they have no known competing financial interests or personal relationships that could have appeared to influence the work reported in this paper.

Received: 23 August 2023 Revised: 27 February 2024 Accepted: 12 March 2024
Published online: 05 July 2024

References

[1] Y Arai, R Inoue, K Goto, et al. Carbon fiber reinforced ultra-high temperature ceramic matrix composites: A review. *Ceramics International*, 2019, 45(12): 14481-14489.
[2] Z L Yang, B Q Li, P C Zhang, et al. Microstructure and thermal physical properties of SiC matrix microencapsulated composites at temperature up to 1900 °C. *Ceramics International*, 2019, 46(4): 5159-5167.
[3] R Penide-Fernandez, F Sansoz. Anisotropic thermal conductivity under compression in two-dimensional woven ceramic fibers foar flexible thermal protection systems. *International Journal of Heat and Mass Transfer*, 2019, 145: 118721.
[4] X C Jin, X L Fan, C S Lu, et al. Advances in oxidation and ablation resistance of high and ultra-high temperature ceramics modified or coated carbon/carbon composites. *Journal of the European Ceramic Society*, 2018, 38(1): 1-28.
[5] Q J Gu, Z Z Quan, J H Yu, et al. Structural modeling and mechanical characterizing of three-dimensional four-step braided composites: A review. *Composite Structures*, 2019, 207: 119-128.
[6] M Y Hao, X Qian, Y G Zhang, et al. Thermal conductivity enhancement of carbon fiber/epoxy composites via constructing three-dimensionally aligned hybrid thermal conductive structures on fiber surfaces. *Composites Science and Technology*, 2023, 231: 109800.
[7] Q W Qiu. Effect of internal defects on the thermal conductivity of fiber-reinforced polymer (FRP): A numerical study based on micro-CT based computational modeling. *Materials Today Communications*, 2023: 106446.
[8] K Dong, J J Zhang, L M Jin, et al. Multi-scale finite element analyses on the thermal conductive behaviors of 3D braided composites. *Composite Structures*, 2016, 143: 9-22.
[9] J A Charles, D W Wilson. A model of passive thermal nondestructive evaluation of composite laminates. *Polymer Composites*, 1981, 2(3): 105-111.
[10] D Bruggemann. The calculation of various physical constants of heterogeneous substances. I. The dielectric constants and conductivities of mixtures composed of isotropic substances. *Annals of Physics*, 1935, 24: 634-664.
[11] M W Pilling, B Yates, M A Black, et al. The thermal conductivity of carbon fibre-reinforced composites. *Journal of Materials Science*, 1979, 14(6): 1326-1338.
[12] H Hatta, M Taya. Effective thermal conductivity of a misoriented short fiber composite. *Journal of Applied Physics*, 1985, 58(7): 2478-2486.
[13] Y Liu, Z G Qu, J Guo, et al. Numerical study on effective thermal conductivities of plain woven C/SiC composites with considering pores in interlaced woven yarns. *International Journal of Heat and Mass Transfer*, 2019, 140: 410-419.
[14] K Dong, K Liu, Q Zhang, et al. Experimental and numerical analyses on the thermal conductive behaviors of carbon fiber/epoxy plain woven composites. *International Journal of Heat and Mass Transfer*, 2016, 102: 501-517.

[15] K Dong, K Liu, L Pan, et al. Experimental and numerical investigation on the thermal conduction properties of 2.5D angle-interlock woven composites. *Composite Structures*, 2016, 154: 319-333.
[16] Y J Xu, S X Ren, W H Zhang. Thermal conductivities of plain woven C/SiC composite: Micromechanical model considering PyC interphase thermal conductance and manufacture-induced voids. *Composite Structures*, 2018, 193: 212-223.
[17] M K Hassanzadeh-Aghdam, M J Mahmoodi, J Jamali. Effect of CNT coating on the overall thermal conductivity of unidirectional polymer hybrid nanocomposites. *International Journal of Heat and Mass Transfer*, 2019, 124: 190-200.
[18] H Huang, Z D Shan, J H Liu, et al. A unified trans-scale mechanical properties prediction method of 3D composites with void defects. *Composite Structures*, 2023, 306: 116574.
[19] X L Shen, X Liu, S J Dong, et al. RVE model with shape and position defects for predicting mechanical properties of 3D braided CVI-SiCf/SiC composites. *Composite Structures*, 2018, 195: 325-334.
[20] K L Wei, J Li, H B Shi, et al. Two-scale prediction of effective thermal conductivity of 3D braided C/C composites considering void defects by asymptotic homogenization method. *Applied Composite Materials*, 2019, 26(5-6): 1367-1387.
[21] H Y Wei, J Zhang, S R Ding. A model for effective thermal conductivity of porous carbon materials in FCM fuel pellets. *Journal of Nuclear Materials*, 2019, 525: 125-139.
[22] L C Zhou, X H Sun, M W Chen, et al. Multi-scale modeling and theoretical prediction for the thermal conductivity of porous plain-woven carbonized silica/phenolic composites. *Composite Structures*, 2019, 215: 278-288.
[23] Z T Guo, H Huang, Z D Shan, et al. A digital implantation system for Z-direction yarn of three-dimensional preform based on flexible oriented woven process. *Engineering Applications of Artificial Intelligence*, 2022, 116: 105385.
[24] Z T Guo, Z D Shan, J H Huang, et al. Study on friction and wear of preform Z-directional fiber. *Polymer Composites*, 2022, 43(5): 2779-2795.
[25] L F Cheng, Y D Xu, L T Zhang, et al. Effect of heat treatment on the thermal expansion of 2D and 3D C/SiC composites from room temperature to 1400 ℃. *Carbon*, 2003, 41(8): 1666-1670.
[26] G E Youngblood, D J Senor, R H Jones, et al. Optimizing the transverse thermal conductivtiy of 2D-SiCf/SiC composites, II. Experimental. *Journal of Nuclear Materials*, 2002, 307-311: 1120-1125.
[27] R Y Luo, T Liu, J S Li, et al. Thermophysical properties of carbon/carbon composites and physical mechanism of thermal expansion and thermal conductivity. *Carbon*, 2004, 42(14): 2887-2895.
[28] J I Múgica, C S Lopes, F Naya, et al. Multi-scale modelling of thermoplastic woven fabric composites: From micromechanics to mesomechanics. *Composite Structures*, 2019, 228: 111340.
[29] T Gereke, C Cherif. A review of numerical models for 3D woven composite reinforcements. *Composite Structures*, 2019, 209: 60-66.
[30] H Huang, Z T Guo, Z D Shan, et al. Prediction of elastic properties of 3D4D rotary braided composites with voids using multi-scale finite element and surrogate models. *Composite Structures*, 2024, 328: 117579.
[31] B Liang, W Z Zhang, J S Fenner, et al. Multi-scale modeling of mechanical behavior of cured woven textile composites accounting for the influence of yarn angle variation. *Composites Part A: Applied Science and Manufacturing*, 2019, 124: 105460.
[32] X H Gao, L Yuan, Y T Fu, et al. Prediction of mechanical properties on 3D braided composites with void defects. *Composites Part B: Engineering*, 2020, 197: 108164.
[33] I Tretiak, R A Smith. A parametric study of segmentation thresholds for X-ray CT porosity characterisation in composite materials. *Composites Part A: Applied Science and Manufacturing*, 2019, 123: 10-24.
[34] L Yang, Y Yan, Z G Ran, et al. A new method for generating random fibre distributions for fibre reinforced composites. *Composites Science and Technology*, 2013, 76: 14-20.
[35] Z Sun, Z D Shan, T M Shao, et al. Numerical analysis of out-of-plane thermal conductivity of C/C composites by flexible oriented 3D weaving process considering voids and fiber volume fractions. *Journal of Materials Research*, 2020: 1-10.
[36] H Z Li, S G Li, Y C Wang. Prediction of effective thermal conductivities of woven fabric composites using unit cells at multiple length scales. *Journal of Materials Research*, 2011, 26(3): 384-394.
[37] J J Gou, Y J Dai, S Li, et al. Numerical study of effective thermal conductivities of plain woven composites by unit cells of different sizes. *International Journal of Heat and Mass Transfer*, 2015, 91: 829-840.
[38] G E Youngblood, D J Senor, R H Jones. Modeling the transverse thermal conductivity of 2-D SiCf/SiC composites made with woven fabric. *Fusion Science and Technology*, 2004, 45: 583-591.

Zheng Sun born in 1989, is a lecturer and a master's supervisor at *Nanjing University of Aeronautics and Astronautics, China*. He obtained his PhD from *Tsinghua University, China*. His main research interests are in the technology and equipment of 3D weaving of advanced composite materials, including the macro, micro, and mesoscale design methods for irregular and complex composite material components, composite forming processes such as braiding, needle punching, and winding, as well as digital forming equipment for large and complex composite material preforms.

Zhongde Shan born in 1970, is a researcher, member of the Chinese Academy of Engineering, and Director of the *State Key Laboratory of Mechanical and Control for Aerospace Structures, China*. He is mainly engaged in the research of digital mechanical equipment and advanced forming manufacturing technology, aerospace manufacturing technology and equipment, and green intelligent manufacturing technology and equipment.

Hao Huang born in 1997, is currently pursuing a PhD degree at *Beijing Institute of Technology, China*. He received his B.E. degree in Mechanical Engineering from *Beijing Institute of Technology, China*, in 2018. His research interests include 3D weaving composites forming, performance prediction and advanced composites equipment.

Dong Wang born in 1997, is currently pursuing a PhD degree at *Beijing Institute of Technology, China*. He received his B.E. degree in Materials from *Harbin Institute of Technology, China*, in 2019, and M.S. degree in Materials Science and Engineering from *China Academy of Machinery Science & Technology*, in 2022. His research interests include 3D weaving composites forming, performance prediction and advanced composites equipment.

Wang Wang born in 1997, is currently pursuing a PhD degree at *Nanjing University of Aeronautics and Astronautics, China*. He received his B.E. degree in Inorganic and Non-metallic Materials Engineering from *Anhui University of Technology, China*, in 2018. His research interests include 3D weaving composites forming, performance prediction and advanced composites equipment.

Jiale Liu born in 1999, is currently pursuing a PhD degree at *Nanjing University of Aeronautics and Astronautics, China*. He received his B.E. degree in Mechanical Engineering from *Nanjing University of Aeronautics and Astronautics, China*, in 2021. His research interests include control of process parameters and shape control for three-dimensional braided preforms.

Chenchen Tan born in 2000, is currently pursuing a PhD degree at *Nanjing University of Aeronautics and Astronautics, China*. She received her B.E. degree in Materials Science and Engineering from *Nanjing University of Aeronautics and Astronautics, China*, in 2022. Her research interests include 3D woven composite weaving and finite element performance prediction.

Chaozhong Chen born in 1985, holds a PhD degree and primarily focuses on the research of high-performance composite materials for rail transit vehicles.